Journal of Petroleum
Science and Technology

Fracture Dynamic Propagation Model of High-Energy Gas Fracturing for Casing Perforated Well

Zhi Yuan Liu[1], Qian Shen Ding[2]*, Bing Zhao[1], De Li[2], and Nan Li[1]

[1] Sinopec Northwest Oilfield Branch, Petroleum Engineering Technology Research Institute, Xinjiang, China

[2] College of Petroleum Engineering, China University of Petroleum, Huangdao Shandong, China

ABSTRACT

The onshore oil and natural gas industries of China have started a large-scale development when crude oil reserves have been difficult to recover. The stratum fracture modification is an indispensable measure to efficiently develop oil and gas fields. Hydraulic fracturing is the most important reservoir stimulation technique, but it is still faced with various problems such as the failure to fracture the target reservoir, long fracturing duration, and short efficient length of the fracture. High Energy Gas Fracturing (HEGF) can easily break down the high-fracture-pressure oil reservoir and generate multiple fractures free of in-situ stress. Moreover, HEGF entails no large-scale devices, and this method is strongly adaptable to the environment without causing environmental pollution. After combining the two technologies (HEGF and the other), then they can complement each other with their strengths. That is, both of them decrease the fracture initiation pressure of (or caused by) hydraulic fracturing on the one hand, and to extend, gather, and support multiple radial fractures of gas fracturing on the other hand. Thus, a fracture zone with a large radius is finally formed, and the percolating resistance of the fluid is significantly decreased.

Moreover, in this study, a dynamic model related to the drainage flow of the perforated holes in a gas well, fluid pressure distribution in the fracture, fluid seepage on the fracture wall, fracture initiation criterion, and fracture propagation velocity during the HEGF process has been presented. Consequently, a gas/liquid/solid coupling fracture dynamic propagation model during the HEGF process can be built to provide a theoretical basis for the accurate simulation of the fracture form changes during this process.

Keywords: High Energy Gas Fracturing, Fracture Dynamic Propagation, Coupling Simulation.

***Corresponding author**
Qian Shen Ding
Email: upcdqs@163.com
Tel: +1 56 2118 9171
Fax: +1 56 2118 9171

Article history
Received: April 10, 2018
Received in revised form: August 13, 2018
Accepted: August 13, 2018
Available online: February 16, 2019
DOI: 10.22078/jpst.2018.3249.1519

INTRODUCTION

Since 2012, there are more than 8,000 high-energy gas fracturing wells in the United States, Canada, Russia, Europe, Africa, Latin America, and the Middle East. The well types also include oil wells, gas wells, water injection wells, and even CBM (Coalbed methane) wells. In addition, Layer types range from low permeability to high permeability sandstone, shale, and limestone. Also, foreign countries generally combine high-energy gas fracturing with perforation, as an auxiliary measure to reduce the pressure loss around the wellbore before hydraulic fracturing, or to unblock the gravel packing well. Most of the charging methods are guns (sleeve type). The main reason for using this method is to ensure that the perforating gun can load enough perforating bullets while it is ensured that the amount of propellant is large enough. In addition, the contamination of the formation is reduced by the perforation.

Fracture dynamic changes during the high energy gas fracturing (HEGF) process is a critical issue during the entire coupling process; therefore, extensive research advancements have been accomplished in the terms of fracture dynamic propagation during the hydraulic fracturing process [1,2]. However, research on the mechanism of high-pressure fluid fracturing rocks during the HEGF process is still insufficient. The relevant calculation models of perforation eyehole drainage flow, fluid pressure distribution within the fracture, fluid seepage on the fracture wall, fracture initiation judgment bases, and fracture propagation velocity are studied based on a systematic investigation of existing research findings.

EXPERIMENTAL PROCEDURES

HEGF Fracture System Physical Model

This study proposes the following hypotheses on the HEGF model based on the relevant theories of fracture propagation analysis under the strong loads of the oil reservoir:

1- The formation is heterogeneous and anisotropic. Anisotropy, also known as “heterogeneity”. All or part of the physical and chemical properties of an object exhibit certain characteristics of the difference which depends on the direction. That is, the performance values measured in different directions are different from each other.

2- The fracture propagation is conformed to or obyed damage mechanics theories. Damage is defined as the process of deterioration of the mechanical properties of the materials or structures caused by the defects of mesostructures under the action of external loads and the environment.

3- The fluid in the fracture forms a one-dimensional stable laminar flow along the fracture length.

4- The cross-section of the fracture width is rectangular; the fracture height remains unchanged, and only the fracture propagation in terms of width and length is considered.

5- The fluid seepage on the fracture wall is considered.

6- The heat conduction during the fracture propagation process is disregarded, but the temperature changes caused by fluid mass transfer are considered.

The fracture propagation schematic diagram based on the preceding hypotheses is shown in Figure 1.

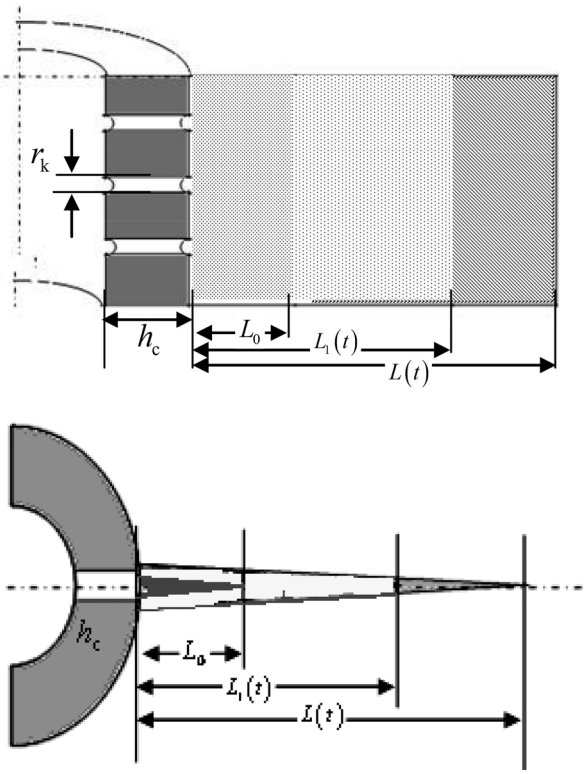

Figure 1: Schematic diagram of the deflagration gas-driven fracture propagation.

In Figure 1, L(t) stands for the total fracture propagation length driven by the high-energy gas, L1(t) is the injection length of the high-energy gas in the fracture, and L_0 is the initial fracture length with a value equal to the perforation length.

The gunpowder of high-energy gas fracturing is generally immersed in a liquid to deflagrate. On the other hand, after detonation, the lower liquid is pushed, or the gunpowder gas is directly squeezed into the hole of the orifice to fracture the oil layer. On the other hand, the upper pressure block is pressed and pushed in the gunpowder of the article. The study of the deflagration model will be simplified to the physical environment shown in Figure 1. Also, within a confined space, the quenching of the gunpowder is quenched, the gunpowder is cylindrical, and the inner surface is simultaneously ignited. The high-energy gas enters the formation through the perforation channel and uses high energy to open the crack.

HEGF Fracture System Mathematical Model

The HEGF fracture dynamic propagation system of the casing perforated well, includes four components; namely, the perforation eyehole, fracture, formation, and high-pressure fluid within (see Figure 1). The fracture propagation process involves the eyehole drainage in the perforation, fluid pressure distribution within the fracture, fluid seepage on the fracture wall, fracture initiation judgment bases, and crack propagation velocity. In addition, the following section presents the dynamics model research on various sub-systems.

Perforation Eyehole Drainage Model

Two methods are used to study the seepage of the high-temperature and high-pressure gas in the perforation eyehole. The first approach is the dimension analysis method proposed by WANG Anshi [3], YANG Weiyu et al [4]. The second approach is the analytical solution proposed by WANG Aihua et al [5]. These approaches are based on nozzle and pipe stream theory of the one-dimensional flow of compressible fluid. Moreover, the current study presents a perforation eyehole drainage model of the gunpowder (or black powder consisting a mixture of sulfur (S), charcoal (C), and potassium nitrate (saltpeter, KNO_3)) fuel gas under the HEGF environment through the second approach. Also, there are some assumptions in this study: (1) the pressure at each point in the construction section of the wellbore is equal; (2) crack height and ground layer thickness are equal; (3) heat exchange between gas and formation does not considered. Equation 1 is as follows:

$$\begin{cases} \dfrac{p_{Tg}}{p} > \left(\dfrac{2}{\gamma+1}\right)^{\frac{\gamma}{\gamma-1}} \text{时} & q_g = nhs_0\left(\dfrac{p-p_1}{\rho_g}\right)^{\frac{1}{\gamma}}\sqrt{\dfrac{2\gamma}{\gamma-1}\dfrac{p_1}{p}\left[1-\left(\dfrac{p_1}{p}\right)^{\frac{\gamma}{\gamma-1}}\right]} \\ \dfrac{p_{Tg}}{p} < \left(\dfrac{2}{\gamma+1}\right)^{\frac{\gamma}{\gamma-1}} \text{时} & q_g = nhs_0\left(\dfrac{p-p_1}{\rho_g}\right)^{\frac{1}{\gamma}}\sqrt{\dfrac{2\gamma}{\gamma-1}\dfrac{p_1}{p}} \end{cases} \quad (1)$$

where q_g is the high pressure gas volume flow rate in m^3/s; P_{Tg} is the gunpowder pressure at the entrance of the outer crack of the casing, MPa×10; P_1 is the outer casing pressure, MPa × 10; n is perforation density, hole / m; h is the height of the crack, cm; S_0 is the cross-sectional area of a hole, cm^2; P is the pressure inside the bubble formed by the combustion product, MPa ×10;γ stands for the polytropic index of the deflagration product, zero dimension, its value is equal to the specific heat ratio k of the gas under adiabatic condition, and it is 1.17 during the constant temperature process; and ρ_g is the density of the gunpowder fuel gas in g/cm^3.

Fluid Flow and Pressure Distribution Model Within the Fracture

After the deflagration fracture initiation, the flow of the high pressure fluid in the fracture can be regarded as the pressing pile flow on a narrow and long cross-section [6]. Respectively, the continuity, momentum conservation, and state equations of the fluid can be built. Through numerical solution, the swelling flow velocity of the fluid in the fracture can be obtained (liquid is driven by gas). However, solving the equation set is a complex process with poor convergence [7,8,10]. Therefore, the studies simplify the fluid pressure within the fracture into a uniform distribution or a trapezoid, triangle equidistribution. The current study considers the pressure attenuation characteristics of the different positions in the fracture, and adopts the pressure distribution model within the fracture provided by the literature [9]. Equation 2 is as follows:

$$p(x,t) = p_1(t)\left(1-\frac{x}{L_1(t)}\right) \quad (2)$$

where P(x,t) is the pressure distribution in Pa within the fracture, $P_1(t)$ is the pressure outside the case (at the root of fracture) at the t moment P, and x is the fracture coordinate calculated from the root of the fracture m.

Seepage of the High Pressure Fluid on the Fracture Wall

The filtration migration of the high-pressure gas in the multi-pore medium is regarded as non-Darcy's seepage [11]. To date, the method is extensively used to describe the phenomenon, and the difference is the item added to Darcy's law [12]. Thereafter, Darcy's law can be changed into Equation 3 as follows:

$$-\frac{\partial p}{\partial l} = \frac{\mu}{K}u(x,t) + \beta\rho\left(u(x,t)\right)^2 \quad (3)$$

where u(x,t) is the seepage velocity in μm^2 of the gunpowder gas on the fracture wall, ρ is the fluid density in kg/m^3 ,β is the non-Darcy's coefficient. Geertsma's method is adopted for calculation [13], and the calculation equation is $\beta=0.005/(K\phi)^{1/2}$ in μm^{-1}. The derivative of $\frac{\partial p}{\partial l}$ expresses the differential form of traffic, cm^3/s; μ is the viscosity of the fluid, mPa·s, and K is the rock permeability.

Thereafter, Both sides of the equation (3) *u(x,t), and its dimension is unified. The equation is as follows:

$$-\frac{\partial p}{\partial t} = 10^9 \times \frac{\mu}{K}\left(u(x,t)\right)^2 + 10^{-6} \times \beta\rho\left(u(x,t)\right)^3 \quad (4)$$

Equation 4 is solved (by us) to obtain the filtration velocity *u(x,t)* at x on the fracture wall coordinate. Also, the value was substituted into Equation 5 to obtain the gas filtration loss of the entire fracture system during the HEGF process within the time period of t.

$$q(t)=\sum_{i=1}^{n}\int_0^t\int_0^{L_{1i}(t)}u(x,t)h\,\mathrm{d}x\,\mathrm{d}t \quad (5)$$

Research on the Fracture Dynamic Propagation Response Model

The fracture dynamic propagation mainly involves three parameters, namely (1) fracture initiation and arrest judgment basis, (2) fracture propagation velocity, and (3) fracture width changes. The conduct of model analysis for each parameter is as follows:

Fracture Initiation and Arrest Judgment Basis

If rocks in the formation are regarded as an elasticity body [14], the Crack Opening Displacement (COD) model typical in the fracture mechanics can be used to analyze the fracture stress model (see Figure 2). The force acting outside the fracture and promoting the closure of the fracture comprises two components.

The first component is the compressional force of the crustal stress on the fracture, while the other is the viscous force causing the stretch damage of rocks on the top end of the fracture.

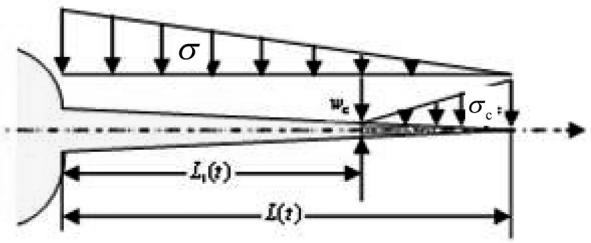

Figure 2: Fracture stress schematic diagram.

The value of the viscous force is decided by the fracture width. The fracture mechanics consider the existence of a critical crack width δ_c. When the fracture width reaches the critical value, the fracture tip will be cracked. The critical width δ_c is an index of the plastic fracture toughness of the material and can be tested through experiment [15]. The literature [16] presents the equation to calculate the critical fracture width as follows:

$$w_c=\frac{2K_{IC}^2(1-\nu)}{\sigma_t} \quad (6)$$

The value of the cohesive form on the top end of the fracture is assumed to constitute a linear distribution [16]. On the top end of the fracture, the viscous force at the zero fracture width is equal to the tensile strength of rocks.

Therefore, the relationship between the viscous force and width of the fracture is shown as follows:

$$\sigma_c(x)=\begin{cases}0 & x<x_c\\ \sigma_t\dfrac{\delta_c-w(x)}{\delta_c} & x\geq x_c\end{cases} \quad (7)$$

where w_c is the critical fracture width m, K_{IC} is the critical stress intensity fracture in Pa*m^1/2 on the top end of the fracture, σ_t is the tensile strength of rocks in MPa, $\sigma_c(x)$ is the plastic viscous force in MPa at x, and x_c is the fracture length coordinate when the fracture width is equal to the critical width δ_c.

The commonly used fracture mechanics theory is adopted based on the stress analysis to conduct a mechanical analysis of the fracture initiation and propagation [14,17]. This theory states that a fracture, with length L, is present on an infinitely large plane; in addition, the general equation for its stress intensity faction is as follows [9]:

$$K_1[\sigma(x,t)]=(\pi L_f(t))^{-\frac{1}{2}}\int_0^L\sigma(x)\sqrt{\frac{L_f(t)+x}{L_f(t)-x}}\,\mathrm{d}x \quad (8)$$

Therefore, the fracture top-end intensity factor that comprehensively considers the crustal stress and fracture top-end viscous force is as follows:

$$K=K_1[\sigma(x,t)]+K_2[\sigma_c(x,t)]+K_3[P(x,t)]$$
$$=(\pi L_f(t))^{-\frac{1}{2}}\int_0^L[p(x,t)-\sigma(x)-\sigma_c(x,t)]\sqrt{\frac{L_f(t)+x}{L_f(t)-x}}\,\mathrm{d}x \quad (9)$$

where K_1 is stress intensity factor (Pa*m$^{1/2}$) and K_2 is intensity factor caused by the cohesion of a

single crack (Pa*m$^{1/2}$). Also, K_3 is Tip stress intensity factor of cracking tendency of high pressure fluid in crack, Pa*m^1/2.

Fracture mechanics theory indicates that the condition for fracture initiation is $K \geq K_{IC}$. That is, when $K \geq K_{IC}$, a fracture initiates. When $K \leq K_{IC}$, a fracture is arrested.

Analysis of the Fracture Propagation Velocity

In this study, once a fracture initiates, it will propagate ahead at a constant velocity as follows [8,9]:

$$v_s = 0.38 C_p \tag{10}$$

where C_P is the velocity of the longitudinal wave, the value of which can be determined by the wave equation $C_P=(E(1-v)/\rho_r(1+v)(1-2v))^{1/2}$ [18], in which v_s is the fracture propagation velocity in m/s, and ρ_r is the rock density in kg/m^3.

Fracture Width Calculation Model

This study adopts the Paris Equation to calculate the fracture opening width as follows [8,19]:

$$W(x,t)=\frac{4(1-\mu)}{G}\int_x^{L(t)}\left[\int_0^{\xi}\frac{p(\zeta,t)-\sigma(\zeta)}{\left(\xi^2-\zeta^2\right)^{1/2}}\mathrm{d}\zeta\right]\frac{\xi}{\left(\xi^2-x^2\right)^{1/2}}\mathrm{d}\xi \tag{11}$$

where G is the rock's shear elasticity in MPa; and ξ and ζ are the instant length during the fracture propagation process and micro-segment length (the microscopic distance in the radial direction at which the crack opens at a certain moment) at the instant m, respectively.

Coupling Solution of the Fracture Dynamic Propagation

The preceding analysis provides the followings: an approximation model for pressure distribution in the fracture, seepage model, stress intensity factor calculation model in the elastic-plastic rock fracture, fracture propagation velocity model, and fracture width model in the high pressure fluid. The combination of these models can facilitate the evaluation if the fracture is propagating at any moment and the description of the fracture forms under the well at any moment during the HEGF process.

The coupling solution process mainly relies on the mass and energy conservation of the high-pressure fluid.

Moreover, the specific solution method is presented as follows:

Mass Conservation Equation

Within a certain time infinitesimal, the flow flowing through the perforation eyehole to the fracture is equal to the sum of the fluid increment within the fracture and flow entering the formation through the fracture wall seepage:

$$\mathrm{d}Q_1 = \mathrm{d}Q_2 + \mathrm{d}Q_3 \tag{12}$$

where dQ_1 is the fluid quality in kg that flows from the perforation eyehole to the fracture within certain time when it is extremely small (or infinitesimal), dQ_2 is the flow in kg that enters the formation through the fracture wall seepage within the time when it is extremely small (or infinitesimal), and dQ_3 is the fluid increment in kg which seeps from the fracture wall to the formation within the time infinitesimal.

Energy Conservation Equation

Ignoring the heat conduction effect during the fracture propagation process, (see Equation 13), the energy dE_1 that flows from the perforation eyehole into the fracture within a certain time when it is extremely small (or infinitesimal) is equal to the sum of the energy increment of the fluid

within the fracture dE_2, fluid energy flowing from the fracture wall to the formation is dE_3, and the energy which is consumed by the fracture opening is dE_4; dE_1 is obtained using the following equation:

$$\mathrm{d}E_1 = \mathrm{d}E_2 + \mathrm{d}E_3 + \mathrm{d}E_4 \tag{13}$$

Coupling Solution

The dynamic model of various sub-systems of the fracture system build up is applied to the mass conservation equation, energy conservation equation, and gunpowder gas fuel equation within the fracture to obtain the numerical solution equation (Equation 14) of the fracture dynamic propagation during the HEGF process:

$$\begin{cases} q(t)\mathrm{d}t = h\int_0^{L_f(t)}\left[\rho(x,t)\dfrac{\partial W(x,t)}{\partial t}\mathrm{d}t + W(x,t)\dfrac{\partial \rho(x,t)}{\partial t}\mathrm{d}t + \dfrac{\partial u(x,t)}{\partial t}\mathrm{d}t\right]\mathrm{d}x \\ \left(\rho_g c_g T_1 + p_w\right)q(t)\mathrm{d}t = c_g T_f\left(\mathrm{d}Q_2(t) + \mathrm{d}Q_3\right) + c_g Q_2(t)\mathrm{d}T_f + \\ h\int_0^{L_f(t)}\left[\left(p(x,t)+\sigma(x,\theta)\right)\dfrac{\partial W(x,t)}{\partial t}\mathrm{d}t + W(x,t)\dfrac{\partial p(x,t)}{\partial t}\mathrm{d}t + p(x,t)u(x,t)\right]\mathrm{d}x \\ p(x,t)M = \rho(x,t)RT_f \end{cases} \tag{14}$$

In Equation 14, the eyehole drainage quantity is q(t), fracture width is W(x,t), seepage velocity on the fracture wall is u(x,t), and pressure distribution P(x,t) along the fracture length is the function of the eyehole entrance pressure (pressure of the fracture root) P_1(x,t) outside the casing. Therefore, the equation set has three unknown numbers, namely P_1(x,t) , T_f, and the density of the gunpowder fuel gas density within the fracture (ρ(x,t)). Moreover, the three equations and three unknown quantities can be quantitatively solved; ρ_g represents the density of the gas (kg/L); R is the molar gas constant of the gas; T is the thermodynamic temperature; c_g is the gas compression factor. M is the molar mass of the gas.

The computational model proposed in this paper comprehensively considers the physical process of coupling multi-factors related to crack propagation in high-energy gas fracturing. In comparison with the fracturing process under single factor, the model has higher precision, and the calculated parameters are closer to the actual situation. Of course, the model is more complicated.

Considering comprehensively, the model requires more parameters, and it is necessary to know the rock property parameters, fluid property parameters, and explosive combustion properties parameters.

The model can be verified based on the comparison of the experimental values and the calculated value curves in the Figure 3.

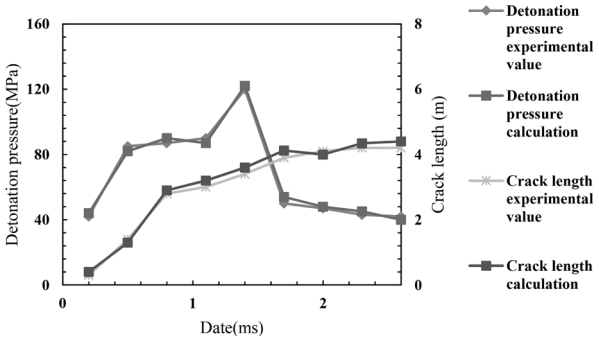

Figure 3: Verify the contrast curve.

During the solution process, formulating the corresponding analytical solution is difficult because of the complexity of the equations involved; thus, the following calculation steps are adopted.

- An analysis is performed to assess whether a fracture propagation exists based on the fracture form and pressure distribution within the fracture at the end of the last moment or not. If fracture propagation exists, then the initial crack form at the moment is calculated. Otherwise, the fracture form of the previous moment is used to calculate the current moment.
- The shaft gunpowder gas pressure P(t) is calculated at the current moment.
- The seepage quantity, fracture length and fracture width based on P(t) and P_1(t-Δt) respectively, and pressure at the root of the fracture of the previous

moment are calculated.

● The fuel gas density within the fracture at the current moment is calculated based on the mass conservation equation.

● The fuel gas state equation is combined to calculate the fluid temperature within the fracture.

● The fuel gas temperature and density within the fracture in the energy conservation equation are used to calculate the pressure at the root of the fracture $P_1(t)$.

● Thereafter, P1(t) is adopted as a new pressure at the root of the fracture. The steps from step 2 are repeated to obtain the pressure $P_1'(t)$.

● In addition, $P_1(t)$ and $P_1'(t)$ are compared. If the error exceeds the scope, then the pressure at the root of the fracture equal to $P_1'(t)$ is used. The calculation is repeated until the error meets the requirement. In addition, the pressure at the root of the fracture $P_1(t)$ is the authentic value of the moment.

● These steps are repeated until the gunpowder completely explodes, and the pressure decreases to the acceptable level to achieve the fracture arrest.

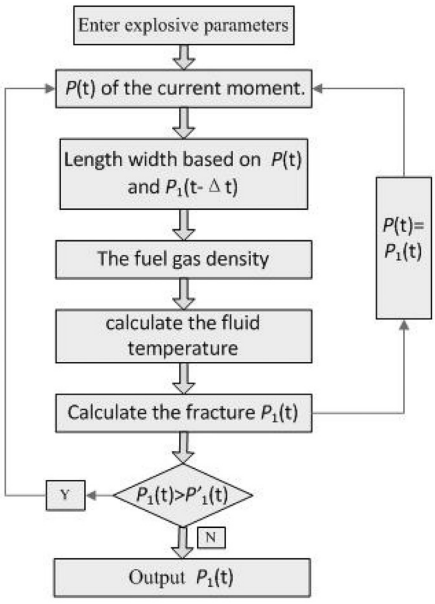

Figure 4: Calculation flow chart.

Case Analysis

Firstly, the parameters related to the stratum are obtained, such as the compressive strength, tensile strength, compressive coefficient and elastic modulus of the formation rock, the viscosity of the fluid, the density, depth and width of the perforation, and the burning speed of the gunpowder. By bringing these parameters into the model, the fluid pressure distribution in the fracture, the fracture initiation standard, and the fracture propagation velocity in the HEGF process can be understood; moreover, the guidance for the actual fracturing process can be provided.

Overview of the Service Well

Chuangao 561 Well is an exploration well at the end of the tectonic axis of Gaomiaozi. The total depth of this well is 5,186.88 m. The oil testing component has two layers, which are located at 4,921 to 4,943.9 m and 4,959 m to 4,995 m respectively. The average porosity is 3.28%, permeability is 0.033×10^{-3} μm^2, and shale content is 9.26%. Moreover, rock density is 2200 kg/m^3, the penetration velocity of the gunpowder gas on the crack wall has been u=16 μm^2, the elastic modulus of the rock has been E=15.5 GPa, the Poisson's ratio v=0.3, the cohesive force has been 6.37 MPa, and the internal friction angle has been 41.72°. Therefore, the reservoir is an abnormally high pressure tight gas reservoir.

After the perforation of Chuangao 561 Well in May 2007, the pilot exploration construction has been conducted directly. The construction curve diagram is shown in Figure 5. After the testing pressure reached 95 MPa, the well started entering the high-squeezing period, and thereby, attempting to crack the formation. However, after three 80-95 MPa vibrations, the formation was not cracked. Moreover,

the flow on the drainage was relatively slow (i.e. approximately 30 m^3 in four days) after perforation and pilot explosion; the natural gas output tested was 0.4507 × 104 m^3/d.

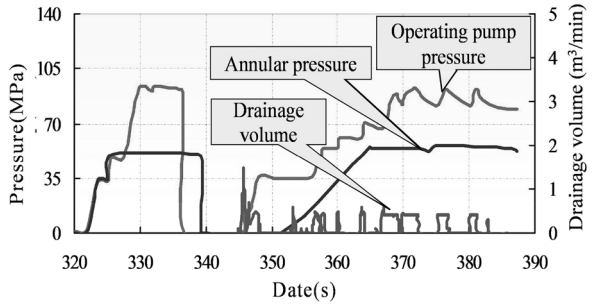

Figure 5: Hydraulic fracturing construction curve of the Chuangao 561 Well.

The analysis of the early-stage measures indicates that the fracturing pressure of the reservoir is abnormally high, which is preliminarily attributed to non-permeation mud pollution. The following actions should be performed to reduce the fracturing pressure of the reservoir: locate the fracture strike of the hydraulic fracturing, increase the yield-increasing effect of the hydraulic fracturing and efficiently protect the casing. Moreover, deflagration fracturing is conducted on the target reservoir to induce fracturing construction.

Analysis of the Construction Process

The deflagration section in this study is from 4,959 m to 4,995 m. The position of the exploder is 4,960 m ± 0.5 m. The parameter optimization proposed here is taken into the model to calculate the fracture strength based on the detonation depth and rock property parameters. The amount of the deflagration material and the density and phase of the perforation are calculated based on the burst strength. After parameter optimization, the propellant mass is 75 kg, hole density is 24 holes/m, perforation phase position is 60°, the piezoresistive fluid backflows at the well entrance, and the fracture bullet adopts the high temperature resistance columnar powder with an outer diameter of 75 mm. Under the parameter combination, the fracture dynamic propagation model built in this study is adapted to calculate the HEGF process. The deflagration pressure change curve and the curve of fracture propagation versus time are predicted (see Figure 6).

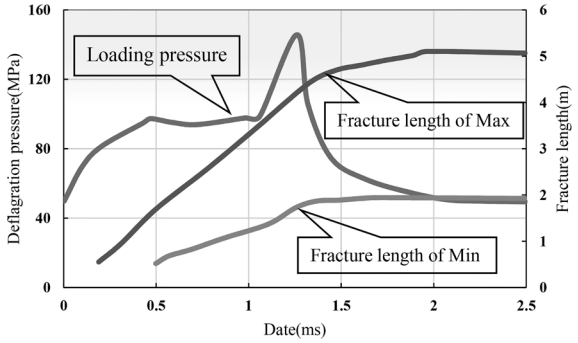

Figure 6: Predicted curve of the deflagration pressure and fracture dynamic propagation.

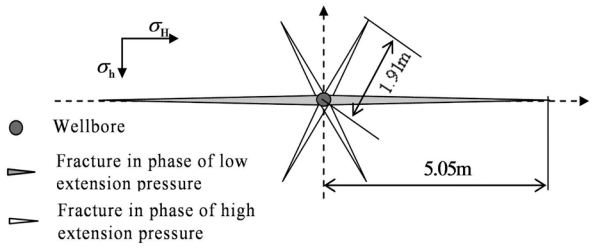

Figure 7: Final fracture form prediction schematic diagram.

After the gunpowder starts deflagration, the system pressure increases and the low circumferential stress phase position fracture begins the propagation (see Figure 6). Along with the increase of the loading pressure of the gunpowder, the high circumferential stress fracture starts propagation, although the propagation velocity is significantly slower than the former. When the gunpowder deflagration is completed, the high and low circumferential stress phase position fracture stops

the propagation, and the HEGF process ends as well. Moreover, the predicted final fracture form is shown in Figure 7.

Analysis of the Measured Effect

When the construction ends, the well is opened for drainage. The three-level flow is adopted for testing and obtaining the construction curve (see Figure 8) [19].

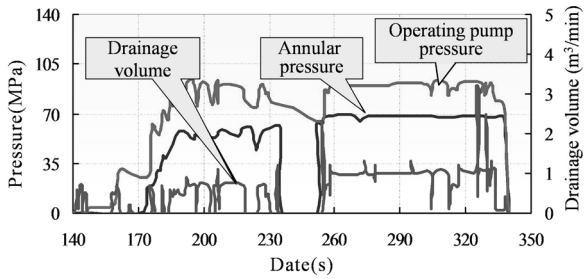

Figure 8: Acid fracturing pre-processing construction curve after fracture induced by the high energy.

A comparative analysis of the test curve before and after the construction has been conducted, and the analysis results were as follows [20]:

(1) HEGF can efficiently reduce the reservoir fracturing pressure and preliminary improve the seepage channel.

After perforation pilot deflagration: construction pumping pressure is 85–95 MPa; displacement is 0.46 m^3/min, and pumping termination pressure is 90.5 MPa (see Figure 3).

After HEGF, construction pumping pressure is 89–92 MPa; displacement is 0.65–0.7 m^3/min, and pumping termination pressure is 76.6 MPa (see Figure 8).

HEGF can efficiently reduce the reservoir fracturing pressure by 13.9 MPa, thereby ensuring the success of the post-stage acid fracturing. The displacement was increased by 46.7% under a similar construction pumping pressure. This way, the seepage channel was preliminarily improved.

(2) Acid fracturing preprocessing measurement can improve the near-well seepage channel.

After the perforation pilot deflagration, the drainage slowed down (i. e. approximately, 30 m^3 in four days) and the natural gas output was measured at 0.4507×10^4 m^3/d.

After the recombined construction, the accumulative total drainage was 70 m^3 in 10 hours, final drainage volume was 110 m^3, and the gas transmission is 7.3×10^4 m^3/d under an oil pressure of 45.5 MPa.

RESULTS AND DISCUSSIONS

Based on the results which have been obtained in this study, the successful acid fracturing pre-processing measure can further improve the seepage channel of the near-well after the HEGF channel is built. The individual well productivity is improved by 16 times and the effect of the measures is guaranteed. The successful implementation of the well stimulation solves the problem of the failure of deep-layer tight gas reservoirs to conduct fracture production. This simulation also ushers in a new total investment and development pattern for Gaomiaozi's south-axis area of the well and other similar oil and gas reservoirs.

CONCLUSIONS

(1) This study built a series of fracture system coupling models, including mathematical models of key parameters, namely eyehole drainage flow, fluid pressure distribution in the fracture, fluid seepage on the fracture wall, fracture propagation judgment bases, fracture propagation velocity, and width changes, involved in the fracture propagation during the HEGF process. Among these models, the fracture propagation judgment basis also considers

the effect of viscous force on the top end of the fracture.

(2) The temperature changes caused by the fluid mass transfer during the deflagration were considered based on the established mathematical model. In addition, the coupling solution equation set of HEGF and its numerical calculation method are proposed based on energy conservation, as well as the energy conservation and gunpowder fuel gas state equations of the entire fracture system which extends from the eyehole drainage flow to the fracture wall.

(3) The success of the pilot experiment of the deflagration-induced acid fracturing in the 561 Well in West Sichuan verifies the feasibility and accuracy of the HEGF model. The results of this experiment can guide the optimal design of HEGF and support the further promotion of the proposed technique.

(4) Through optimal parameter design and successful implementation of HEGF in Chuangao 561, as well as the analysis of the measured effect, acid fracturing can hardly squeeze the liquid acid into the deep formation layer in the deep, tight gas, and high fracturing pressure formation. Moreover, HEGF can efficiently reduce the formation fracturing pressure, thereby ensuring the smooth progress of hydraulic fracturing or acid fracturing. Moreover, HEGF can use the induced fractures free of the control of the crustal stress to expand the seepage area and improve the efficiency of the well stimulation.

ACKNOWLEDGMENTS

The authors acknowledge the support by the Fundamental Research Funds for the Central Universities (FRFCU) through the "Numerical simulation study on influence of low-frequency resonant wave on percolation in low permeability reservoir" project (Project Number: 16CX02020A); the Natural Science Foundation of China (NSFC) through the project named "Research on complex oil displacement mechanism of low-frequency vibration and surfactant for low permeability reservoir" (Project Number: 51274229) and «the Kinetic Mechanism Study of Delay Time Controlled High Energy Gas Fracturing» (Project Number: 51104173).

NOMENCLATURES

CBM	: Coalbed methane
HEGF	: High Energy Gas Fracturing
COD	: Crack Opening Displacement

REFERENCES

1. Wang H. X. and Zhang S. C., "Numerical Calculation Methods for Hydraulic Fracture Design," *Petroleum Industry Press*, **1998**, *6*, 108-118.
2. Zhang Q., "Principle and Design of Oil Production Engineering," *University of Petroleum Press*, **2005**, *6*, 259-260.
3. Wang A. S. and Qin F. D., "High Energy Gas Fracturing Techniques," *Northwest University Press*, **1998**, *10*, 70-77 .
4. Yang W. Y., Zhou C. H., and Zhao G., "An Analysis of Coupled Transient Pressure during High Energy Gas Fracturing (HRGF)," *Acta Petrolei Sinica*, **1993**, *14*(3), 127-134.
5. Wang A. H., Li D., and Zhao F. L., "The Study of Number of Fractures using High Energy Gas Fracturing Model," *Duankuai Youqitian*, **2000**, *7*(5), 56-59.
6. Wang B. G., Liu S. Y., and Huang W. G., "Gas Dynamics," *Institute of Technology Press*, **2005**, *8*, 184-188.

7. Yang X. L. and Wang M.S., "Mechanism of Rock Crack Growth under Detonation Gas Loading," *Explosion and Shock Waves*, **2001**, *21*(2), 111-116.
8. Lu W. B. and Tao Z. Y., "A Study of Fracture Propagation Velocity Driven by Gases of Explosion Products," *Explosion and Shock Waves*, **1994**, *14*(3), 264-267.
9. Chen L. J., Li N., and Wang J. Q., "Initiation and Extension of Existing Cracks under Detonation Gas Loading in a High Energy Combined Perforation," *Petroleum Exploration and Development Journal*, **2005**, *32*(6), 93-120.
10. Nilson R. H., Proffer W. J., and Duff R, E. "Modeling of Gas Driven Fractures Induced by Propellant Combustion within a Borehole. International Journal of Rock Mechanics," *Mining Science and Geomechanics*, **1985**, *22*(1), 3-19.
11. Zhang L. H., Zhu S. Q., and Wang K., "Adsorption Equilibrium Model and its Verification of Gas Mixture," *Xinjiang Petroleum Geology*, **2004**, *25*(2), 165-167.
12. Cornell D. and Katz D. L., "Flow of Gases through Consolidated porous Media," *Industrial and Engineering Chemistry*, **1953**, *45*, 2145.
13. Geertsma J., "Estimating the Coefficient of Inertial Resistance in Fluid Flow through Porous Media," *Society of Petroleum Engineers Journal*, **1974**, *10*, 445-450.
14. Atkinson B. K. "Fracture Mechanics of Rock" (Translation)," *Seismological Press*, **1992**, 57-62.
15. Li Y. D., "Theory and Application of Fracture Mechanics," *China North Industries Group Press*, **2005**, *11*, 82-83.
16. George E., Zacharias A., and Eleftherios L., "Effect the Fracture Process Zone in Directed Crack Propagation in Borehole Blasting," *Society of Petroleum Engineers*, **1994**, SPE-28085-MS, Netherlands, 463-447.
17. Cao Y. G., Liu C. S., and Lin P. "Establishing the Model for Calculating the Fracturing Pressure of Formation Rock during Oil/gas Wells Fracturing by Using Fracture Mechanics Theory," *Journal of Xian Petroleum Institute (Natural Science Edition)*, **2003**, *18*(4), 36-39.
18. Zhang Z. C., "The Crack Expansion of Controlled Blasting for Rock Fracture," *Journal of Southwest Institute of Technology*, **2000**, *15*(1), 60-66.
19. Tada H., Paris P. C., and Irwin G. R., "The Stress Analysis of Crack Handbook," Del Research Corporation Hellertown, **1973**.
20. Wu F. P., Pu C. S., and Ren S., "Pilot Test of Blasting-acid Fracturing Complex Technology in Gas Wells of Western Sichuan," *Journal of China University of Petroleum*, **2008**, *32*(6), 101-103.